Evolution of Magnetic and Lattice Interactions with Hole and Electron Doping in Perovskite Cobaltites

Juan Yu[1], Peng Tong[1], Daniel Phelan[2] and Despina Louca[1]

[1]Dept. of Physics, University of Virginia; [2]NCNR, NIST

Spin-state transitions in $LaCoO_3$

The ground state of $LaCoO_3$ is nonmagnetic and insulating, but the Co^{3+} ion is easily excited from the low spin state (LS=0, $t_{2g}^6e_g^0$) to an excited state (IS=1, $t_{2g}^5e_g^1$ or HS=2, or $t_{2g}^4e_g^2$) upon warming at ~ 100 K. Using inelastic neutron scattering we previously witnessed this spin-state transition by observing an associated excitation at ~ 0.6 meV, which corresponds to a spin-flip transition within the S=1 energy manifold [1].

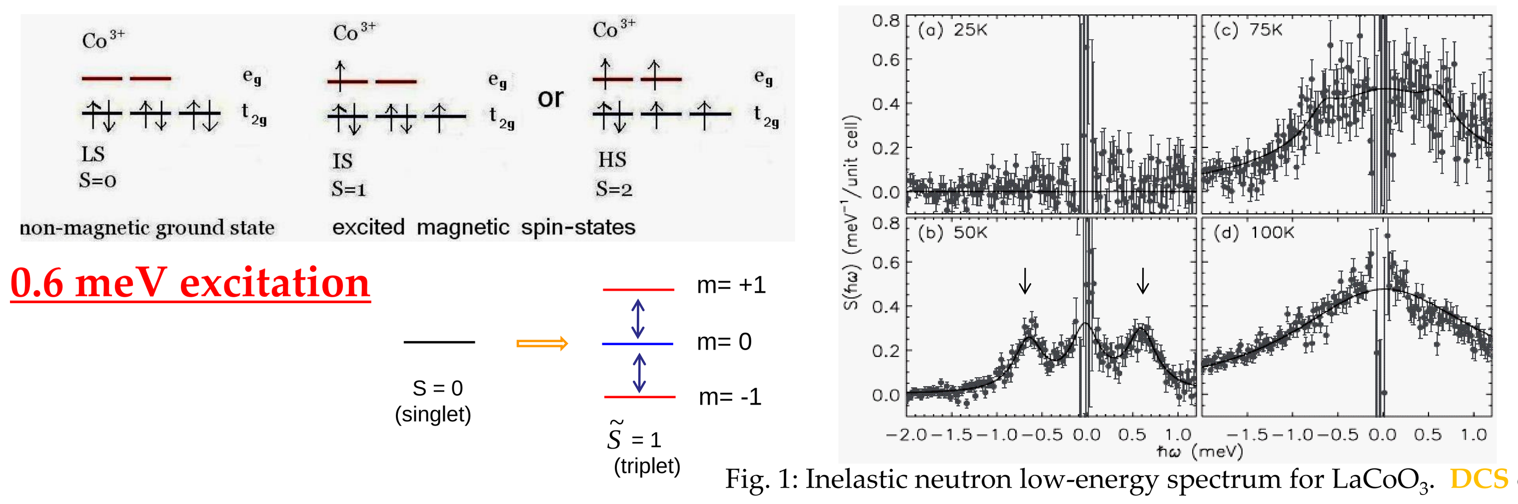

Fig. 1: Inelastic neutron low-energy spectrum for $LaCoO_3$. DCS data

Hole-doping effects in $La_{1-x}A_xCoO_3$ (A= Ca^{2+}, Sr^{2+} or Ba^{2+})

Magnetic phase separation in Sr and Ba doping [2, 3]

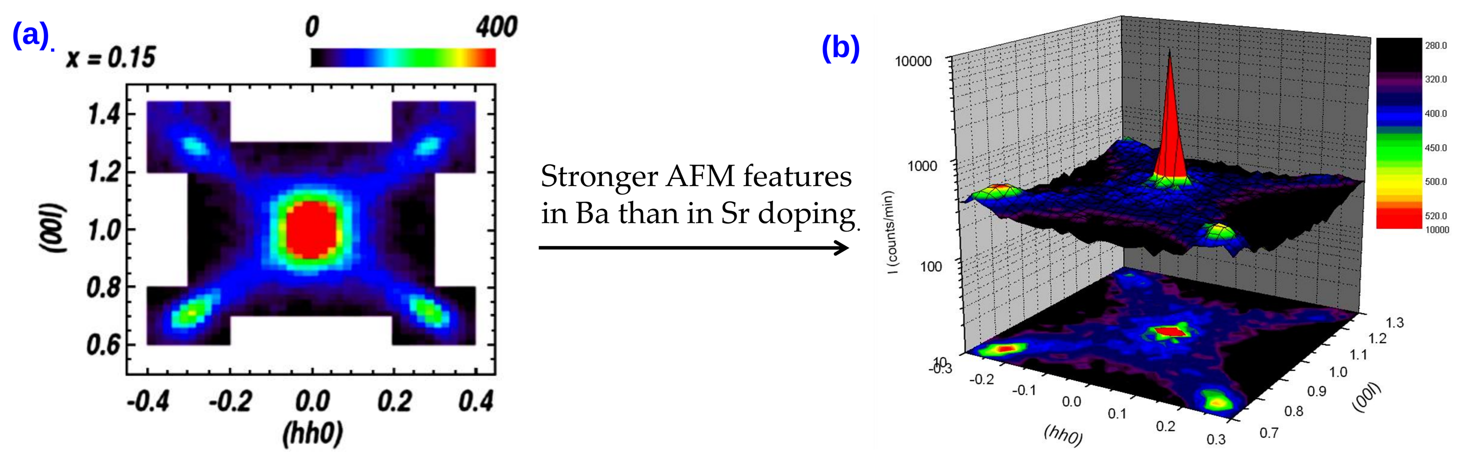

Fig. 2: (a) and (b) are elastic neutron scattering contour maps in (hhl) plane for $La_{0.85}Sr_{0.15}CoO_3$ and $La_{0.9}Ba_{0.1}CoO_3$ at low temperature, respectively. The center (001) peak contains both nuclear and magnetic components while the broadening around the peak indicates short-range FM correlations. Four satellite peaks appear at incommensurate positions with the lattice periodicity with Sr doping, but at commensurate positions with Ba doping. The data are obtained from the SPINS.

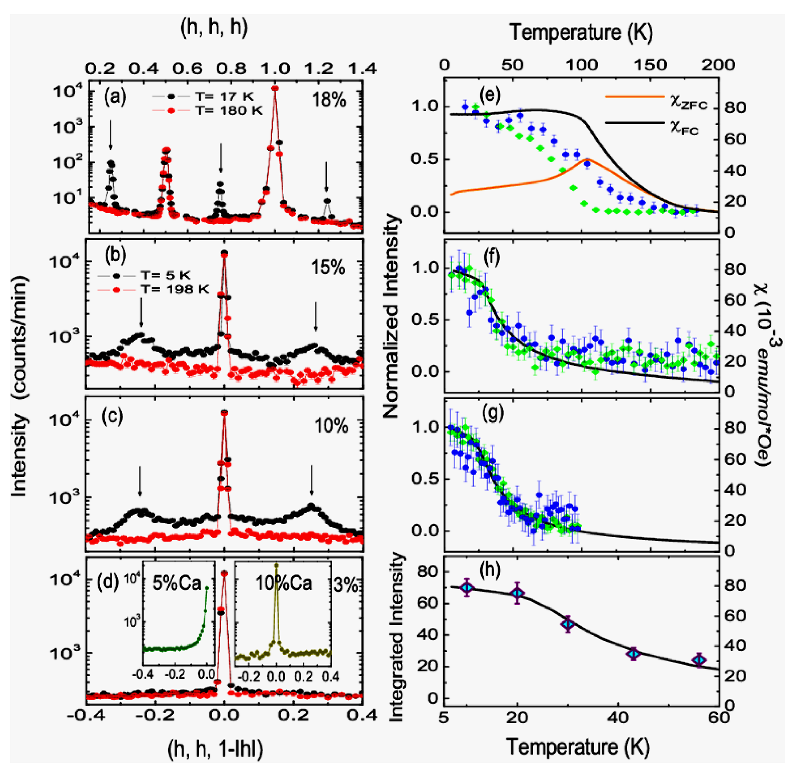

Fig. 3: (a) The scans along (h,h,h) shown for (a) x = 0.18 were collected at TOPAN, and along (h,h,1-|h|) for (b) 0.15, (c) 0.10, and (d) 0.03 of the Ba crystals, and 5 and 10 % Ca shown in the inset of (d) which were collected at SPINS. (e)-(f) are the order parameters of the satellite (green) and ferromagnetic (blue) components, compared to FC bulk. (h) is the integrated intensity for the x = 0.10 and compares well with bulk.

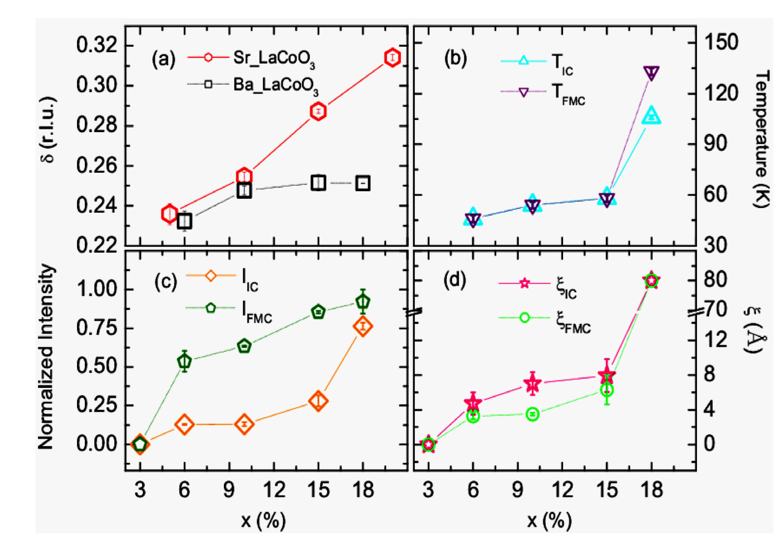

Fig. 4: (a) is a plot of the IC peak position of Ba compared with Sr crystals as a function of x %. (b) is a plot of the order parameter for the two magnetic phases. (c) is a plot of the normalized satellite peak intensity and the (001) Bragg peak. (d) is a plot of a comparison of the IC and FMC correlation lengths. Note that it is comparable in the two magnetic phases for all x, while the value of 80 Å for the 18 % is a lower bound limit due to the experiment resolution.

- Competing FM and AFM phases develop with doping.
- AFM phase is enhanced with increase of the ionic size at the A-site.

A structurally driven magnetic phase transition in Ba [4]

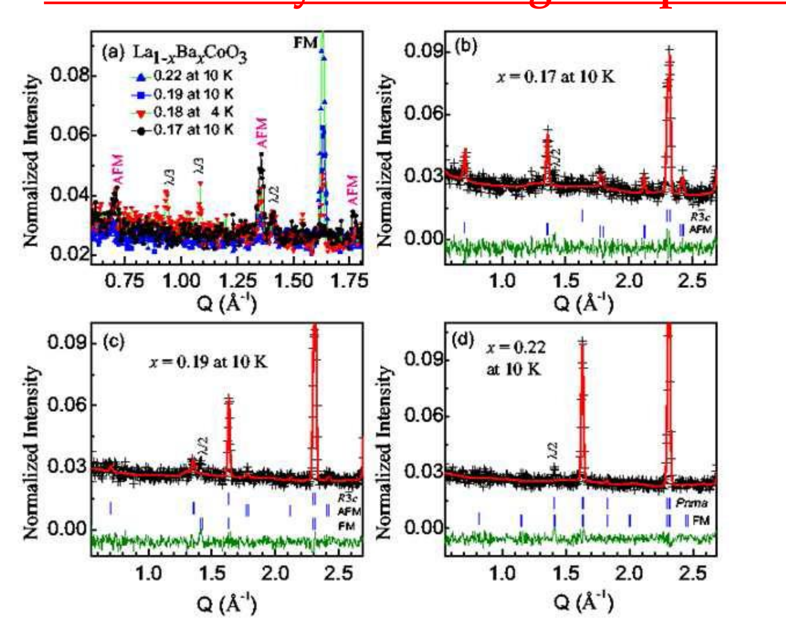

Fig. 5 The neutron diffraction patterns obtained from BT-1 for x = 0.17 to 0.22. The observed intensities are plotted as symbols (cross) and the calculated patterns as solid lines.

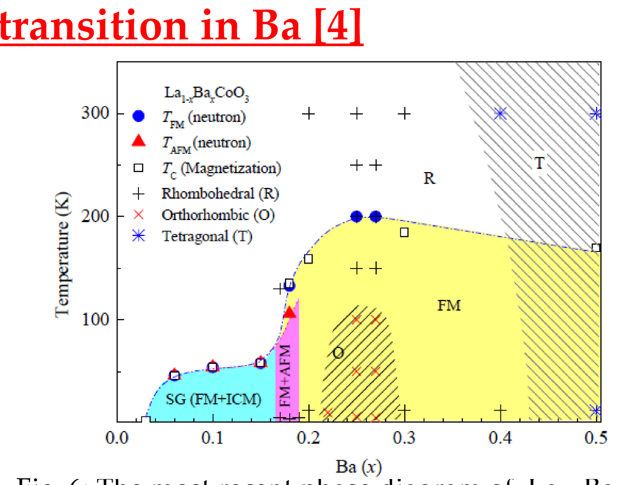

Fig. 6: The most recent phase diagram of $La_{1-x}Ba_xCoO_3$

- In Ba doped cobaltites, the crystal structure and magnetic structural transitions are strongly coupled.
- A very rich phase diagram is revealed in the Ba system.

Electron doping effects in $LaCo_{1-y}B_yO_3$ (B= Ni^{3+}, Fe^{3+} [5])

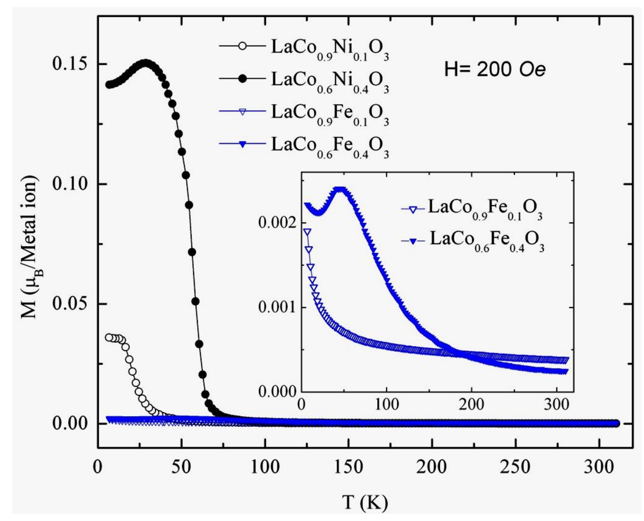

Fig. 7: The temperature dependence of field-cooled magnetization for $LaCo_{1-y}B_yO_3$ at H= 200 *Oe*.

The bulk properties change dramatically with electron doping:

- With Ni, the system transforms from a spin-glass to a ferromagnet at y~ 10 % and to a metal at y~ 40 %.
- With Fe, the system remains in a paramagnetic-like state up to y~ 40%, and then becomes AFM.

From our atomic structure studies, we find that the lattice responds to Ni and Fe doping in different ways, beyond steric effects.

Two effects on the oxygen octahedron of trigonal distortions ($R\bar{3}c$)

ω: rotation of the octahedron around [111]

ζ: octahedral strain along [111]

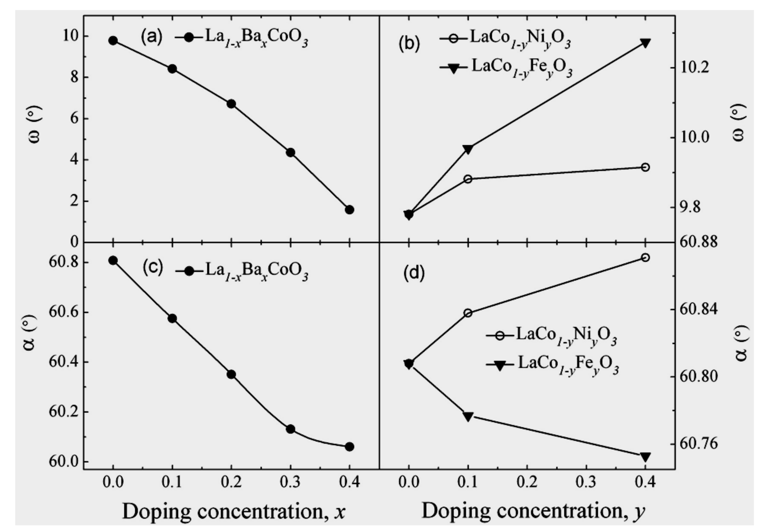

Fig. 8: The Rietveld refinement results at RT of the rhombohedral unit cell angle, α, and the $BO_{6/2}$ rotation, ω, as a function of concentration for $La_{1-x}Ba_xO_3$ in (a) and (c), for $LaCo_{1-y}Ni_yO_3$ and $LaCo_{1-y}Fe_yO_3$ in (b) and (d), obtained from the NPDF.

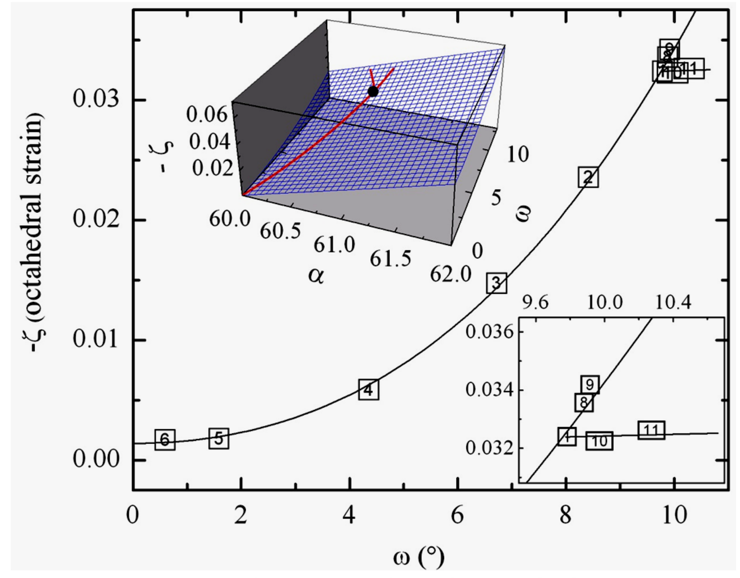

Fig. 9: ζ as a function of ω for $LaCoO_3$ (#1); $La_{1-x}Ba_xCoO_3$ (#2 - 6 for x = 0.1 - 0.5); $LaCo_{1-y}Ni_yO_3$ (#8 and 9 for x = 0.1 and 0.4); and $LaCo_{1-y}Fe_yO_3$ (#10 and 11 for y = 0.1 and 0.4). The black line is an empirical fit for Ba doped samples. The inset at the upper corner is a plot of ζ in the ω - α phase space. The inset at the lower corner is an expansion of the high ω region.

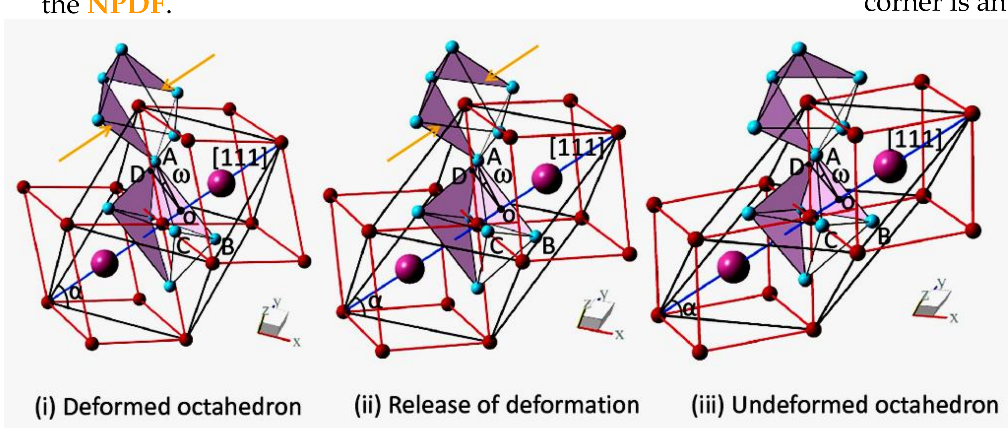

Fig. 10: For a given oxygen displacement *x*, i.e. for a given ω, (i) shows the octahedral deformation when α > 60°, (ii) when α ~ 60° and (iii) when α < 60°. To maintain the regular shape of the octahedron, α has to be smaller than 60. Otherwise, a compression is applied along the trigonal axis shown here with the orange arrows.

Both Ni and Fe compounds are in $R\bar{3}c$ but

- Ni doping increases ω and ζ.
- Fe doping only increases ω.

The absence of Co-O bond splitting

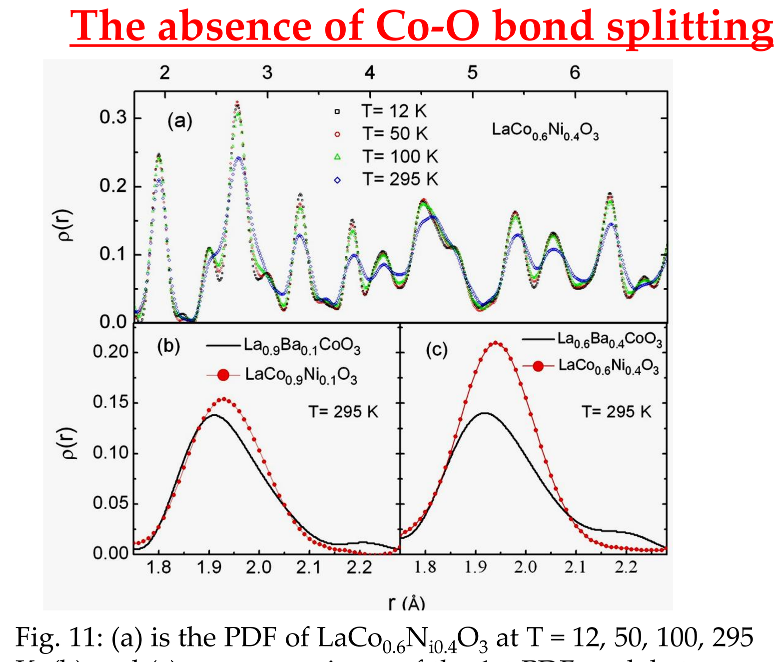

Fig. 11: (a) is the PDF of $LaCo_{0.6}Ni_{0.4}O_3$ at T = 12, 50, 100, 295 K. (b) and (c) are comparisons of the 1st PDF peak between $LaCo_{1-y}Ni_yO_3$ and $La_{1-x}Ba_xCoO_3$ for x = y = 10 % and 40 % at 295 K, respectively, measured using NPDF.

The absence of AFM correlations

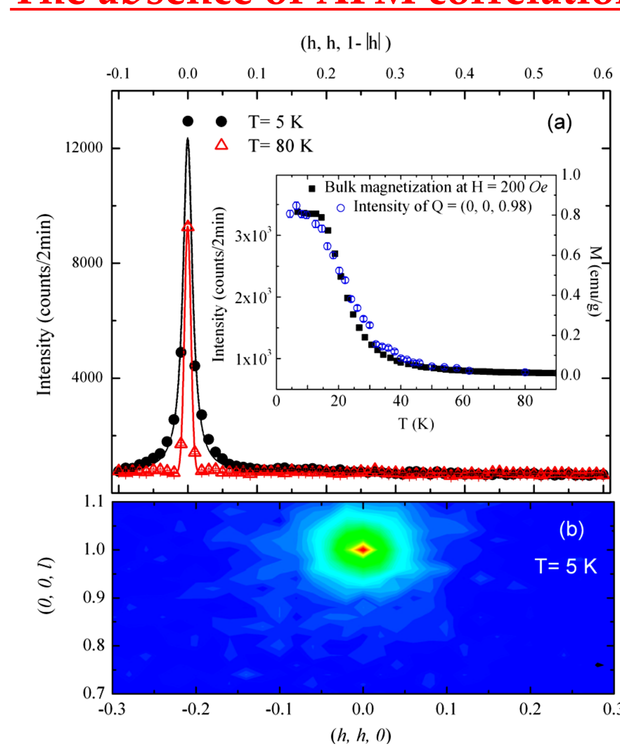

Fig. 12: (a) The elastic scattering along (h, h, 1 - |h|) for a $LaCo_{0.9}Ni_{0.1}O_3$ single crystal. A broad intensity due to magnetic scattering at low temperatures only appears around the (001) Bragg peak. (b) an elastic contour map in the (hhl) plane, measured at SPINS.

- Hole doping with Sr/Ba releases the trigonal distortion significantly, while in the local structure, two distinct Co-O bonds are identified, indicating the existence of the IS state of Co^{3+} ion.
- Ni and Fe doping both increase the octahedral rotation but only in Ni is it accompanied by a compression along the trigonal axis. This distortion is invoked to break the degeneracy of the magnetic Co^{3+} ions, which most likely are in the hish-spin state, while keeping the Co-O bonds at constant length.
- The absence of the AFM correlations in Ni doping implies that the magnetic exchange is not simply superexchange.

Dilute electron-doping effects in $LaCo_{1-y}B_yO_3$ [6]

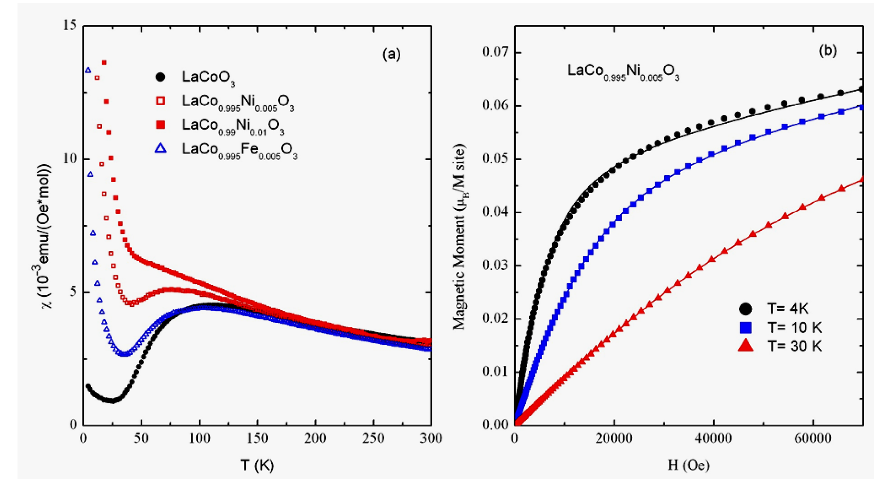

Fig.13: (a) the bulk magnetic susceptibility as a function of temperature for lightly Ni and Fe doped samples compared with pure compound. (b) the field dependence of $LaCo_{0.995}Ni_{0.005}O_3$. The lines are the fits to a modified Brillouin function.

- The Curie-like χ is more obvious with Ni doping than with Fe doping which is counter intuitive (S_{Fe3+} =5/2 vs. S_{Ni3+} =1/2).
- The fitting by a modified Brillouin function gives rise to a large total spin *g*S ~ 20 μ_B associated with each Ni dopant, indicating some Co^{3+} may become magnetic down to T = 0 K.

A new excitation at ~ 1.1 meV

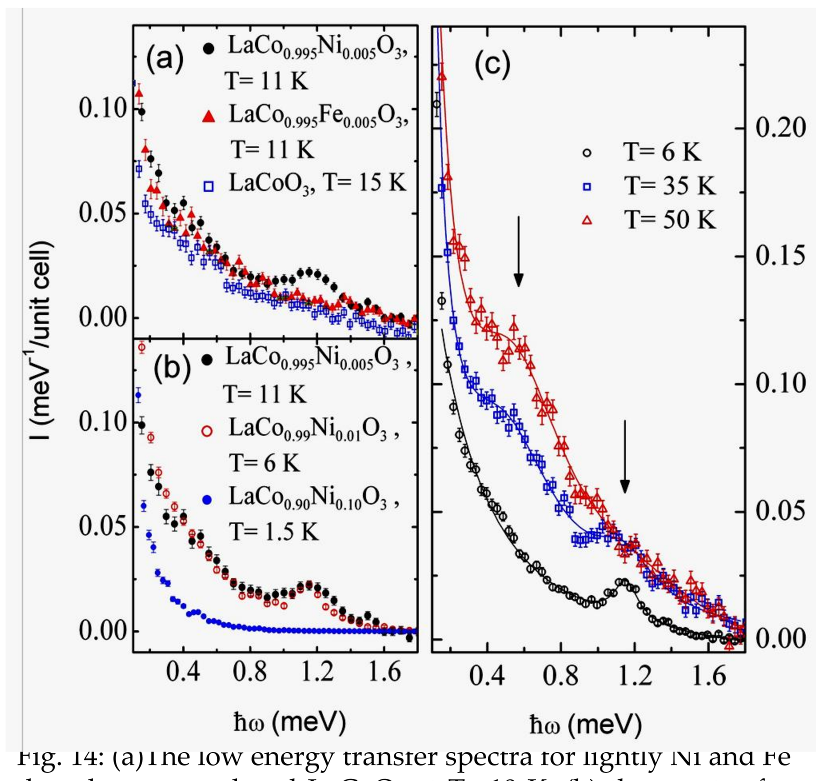

Fig. 14: (a) The low energy transfer spectra for lightly Ni and Fe doped compound and $LaCoO_3$ at T~ 10 K. (b) the spectra for Ni doping of y= 0.005, 0.01 and 0.1. (c) the temperature dependence of the spectra for $LaCo_{0.99}Ni_{0.01}O_3$. DCS data.

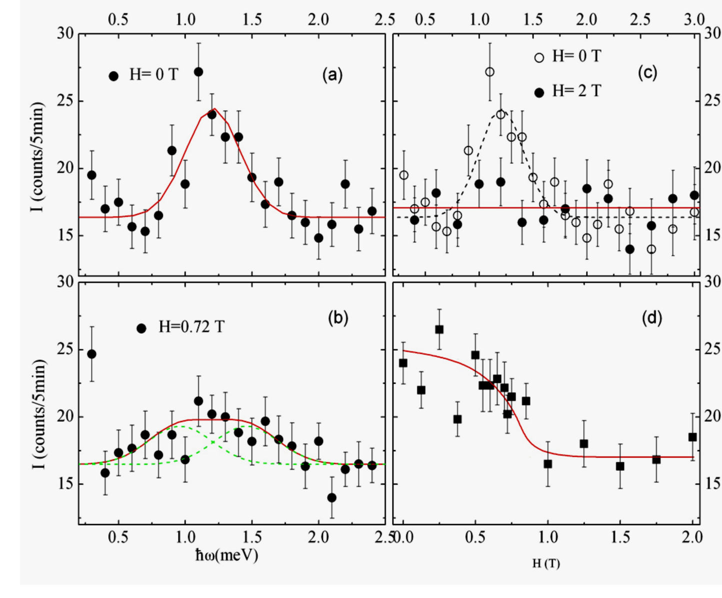

Fig.15: The field dependence of the excitation at low temperature. The broadening of the peak under field can be due to peak splitting, fit by two Gaussian functions. The data are obtained from the SPINS.

A possible carrier induced FM

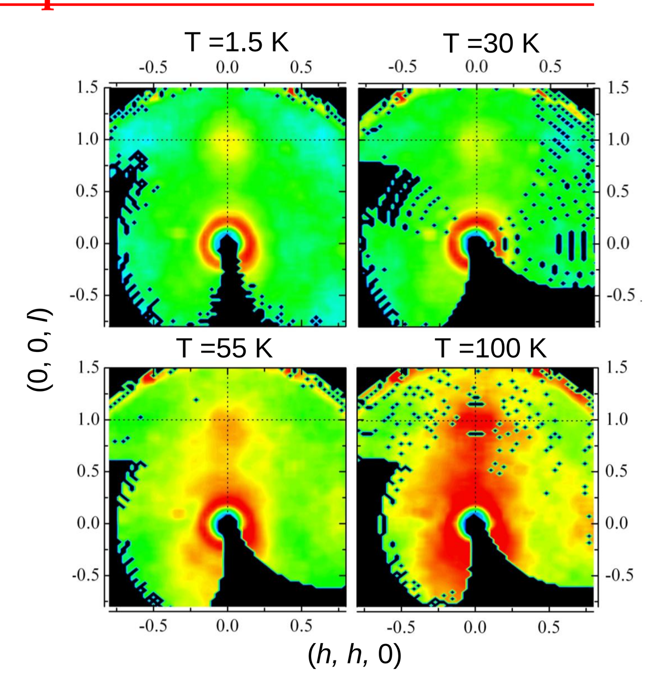

Fig. 16: The inelastic neutron contour maps at the constant energy transfer ΔE= 1.1 meV in (hhl) plane showed the Q-dependence of the excitation in $LaCo_{0.995}Ni_{0.005}O_3$ single crystal at different temperatures, measured on MACS.

- The new excitation at ~ 1.1 meV appears only in the paramagnetic state of Ni doping.
- Present below ~40 K.
- It responds to the applied field confirming its magnetic nature.
- It is only associated with short-range ferromagnetic coupling.
- The exchange interactions are weak and may be mediated by the dilute carriers provided by the mobile Ni spins through an RKKY-like mechanism.

Summary

- Due to the nearly degenerate spin states of the Co^{3+} ion in $LaCoO_3$, spin-state transition can be easily driven thermally as well as by hole doping at the A-site or electron doping at the B-site.
- The hole doped systems exhibit rich phase diagrams with magnetic phase separation, metal-insulator transitions, and strong magneto-elastic coupling coupled to structural transitions.
- The electron doped systems have been largely unexplored. The magnetic interactions appear to be more complex, not simply understood by Double or Super-exchange.

References

[1] D. Phelan, D. Louca, *et al.*, *Phys. Rev.* L **96,** 027201 (2006).
[2] D. Phelan, D. Louca, *et al.*, *Phys. Rev.* L **97,** 235501 (2006).
[3] J. Yu, D. Louca, *et al.*, *Phys. Rev.* B **80,** 052402 (2009).
[4] P. Tong, J. Yu, D. Louca *et al.*, *Phys. Rev.* L (2011).
[5] J. Yu, D. Louca *et al.*, *Phys. Rev.* B **82**, 224101 (2010).
[6] J. Yu, D. Louca *et al.*, in preparation.

Acknowledgment: This work has been carried out under the auspices of the Department of Energy under contract DE-FG02-01ER45927.